

Research Article

Synthesis and Evaluation of Amino Acid-Based Radiotracer ^{99m}Tc -N4-AMT for Breast Cancer Imaging

Fan-Lin Kong, Mohammad S. Ali, Yinhan Zhang, Chang-Sok Oh, Dong-Fang Yu, Mithu Chanda, and David J. Yang

Department of Experimental Diagnostic Imaging, The University of Texas M. D. Anderson Cancer Center, 1515 Holcombe Boulevard, Houston, TX 77030, USA

Correspondence should be addressed to Fan-Lin Kong, fanlin.kong@mdanderson.org

Received 30 December 2010; Accepted 14 February 2011

Academic Editor: Lie-Hang Shen

Copyright © 2011 Fan-Lin Kong et al. This is an open access article distributed under the Creative Commons Attribution License, which permits unrestricted use, distribution, and reproduction in any medium, provided the original work is properly cited.

Purpose. This study was to develop an efficient synthesis of ^{99m}Tc -O-[3-(1,4,8,11-tetraazabicyclohexadecane)-propyl]- α -methyl tyrosine (^{99m}Tc -N4-AMT) and evaluate its potential in cancer imaging. **Methods.** N4-AMT was synthesized by reacting N4-oxalate and 3-bromopropyl AMT (N-BOC, ethyl ester). *In vitro* cellular uptake kinetics of ^{99m}Tc -N4-AMT was assessed in rat mammary tumor cells. Tissue distribution of the radiotracer was determined in normal rats at 0.5–4 h, while planar imaging was performed in mammary tumor-bearing rats at 30–120 min. **Results.** The total synthesis yield of N4-AMT was 14%. Cellular uptake of ^{99m}Tc -N4-AMT was significantly higher than that of ^{99m}Tc -N4. Planar imaging revealed that ^{99m}Tc -N4-AMT rendered greater tumor/muscle ratios than ^{99m}Tc -N4. **Conclusions.** N4-AMT could be synthesized with a considerably high yield. Our *in vitro* and *in vivo* data suggest that ^{99m}Tc -N4-AMT, a novel amino acid-based radiotracer, efficiently enters breast cancer cells, effectively distinguishes mammary tumors from normal tissues, and thus holds the promise for breast cancer imaging.

1. Introduction

^{18}F -fluoro-deoxy-glucose (FDG), an ^{18}F -labeled glucose analog, is the most common radiotracer for positron emission tomography (PET) in cancer diagnosis [1]. However, FDG-PET has several limitations in practice, for example, FDG cannot distinguish tumor tissues from inflammatory or normal brain tissues. Therefore, ^{18}F -labeled amino acid-based radiotracers have been reported as an alternative, which is based on the fact that tumor cells take up and consume more amino acids to maintain their sustained fast growth. Among those radiotracers, ^{18}F -labeled α -methyl tyrosine (AMT) has shown high tumor uptake and great ability to differentiate tumor tissue from inflammatory sites in brain tumors and squamous cell carcinoma [2]. ^{18}F -AMT enters the tumor cells via L-type amino acid transporters (LAT), which is the only system that can transport large neutral amino acids with aromatic rings [3]. LAT, especially its subtype LAT1, was reported to be highly expressed in many cancer cell lines and positively correlates with tumor growth [4, 5]. So far, ^{18}F -AMT is the most suitable amino

acid transporter-targeting radiotracer for tumor imaging, regardless of low synthesis yield and requirement of an on-site cyclotron to produce ^{18}F .

Although PET has emerged as an advanced imaging tool for cancer diagnosis, only limited facilities around the world can afford complete armamentarium of PET and cyclotron for the local production of short-lived positron-emitting radionuclides such as ^{11}C and ^{18}F . Therefore, mature technologies, that is, single photon emission computed tomography (SPECT) or its combination with computed tomography (CT), still play important and irreplaceable roles in nuclear imaging area [6]. The most common radionuclide for SPECT is technetium-99m (^{99m}Tc , $t_{1/2} = 6.02$ h), which is produced by in-house generator and does not require the cyclotron [7]. Due to their similar chemistry, the diagnostic radioisotope ^{99m}Tc and the therapeutic radioisotope rhenium-188 (^{188}Re) could be labeled to the same ligand, which leads to the diagnostic/therapeutic matched pair. Unlike most of the cyclotron-produced radionuclides that utilize the covalent chemistry for labeling, ^{99m}Tc requires a “chelator” to conjugate the radionuclide with the target ligand. The nitrogen,

oxygen, and sulfur combinations have been shown to be stable chelators for ^{99m}Tc such as N_4 (e.g., DOTA, cyclam-14), N_3S (e.g., MAG-3), N_2S_2 (e.g., ECD), NS_3 , S_4 (e.g., sulfur colloid), diethylenetriamine pentaacetic acid (DTPA), O_2S_2 (e.g., DMSA), and hydrazinonicotinamide (HYNIC) [8–13].

Here, we report the synthesis of precursor O-[3-(1,4,8,11-tetraazacyclotetradecan)-propyl]- α -methyl tyrosine (N_4 -AMT) and its radiolabeling with ^{99m}Tc . *In vitro* cellular uptake kinetics and planar scintigraphic imaging of ^{99m}Tc - N_4 -AMT were also evaluated.

2. Materials and Methods

All chemicals of analytical grade and solvents of HPLC grade for compound synthesis were purchased from Sigma-Aldrich (St. Louis, MO). ^1H -, ^{13}C -NMR spectra were performed on Bruker 300 MHz spectrometer in CDCl_3 , CD_3OD , and D_2O . Tetramethylsilane was used as an external standard. Chemical shifts were reported in δ (ppm) and J values in hertz. Sodium pertechnetate ($\text{Na}^{99m}\text{TcO}_4$) was obtained from $^{99}\text{Mo}/^{99m}\text{Tc}$ generator in Mallinckrodt (Houston, TX).

2.1. Synthesis of Precursor N_4 -AMT

2.1.1. α -Methyl Tyrosine Ethylester 2. The synthetic strategies for precursor N_4 -AMT are demonstrated in Figure 1. Thionyl chloride (10 mL; 137.42 mmol) was added to a solution of α -methyltyrosine **1** (10.00 g; 51.22 mmol) in anhydrous ethanol (60 mL) at 0°C , and then heated at 78°C for 4 h while stirring. After cooling, the reaction mixture was reduced to 20 mL, and then 10 mL of triethylamine was added into it. The mixture was poured into 100 mL of water and extracted with chloroform. The combined organic layers were dried over MgSO_4 and evaporated. The desired compound was obtained as white solid. Yield: 9.00 g (40.32 mmol, 78.75%). ^1H -NMR (CDCl_3) δ = 7.02 (d, 2H, J = 8.4 Hz), 6.70 (d, 2H, J = 8.4 Hz), 4.22 (dd, 2H, J = 7.2 Hz, J = 7.8 Hz), 3.14 (dd, 2H, J = 13.5 Hz, J = 13.5), 1.42 (s, 3H), 1.33 (t, 3H, J = 16.2 Hz) ppm. ^{13}C -NMR δ = 175.47, 156.36, 130.66, 126.39, 114.87, 61.05, 58.65, 45.29, 24.08, 13.07 ppm, MS: m/z = 224.23 [M] $^+$.

2.1.2. N -*t*-Butoxycarbonyl- α -Methyl Tyrosine Ethylester 3. Compound **2** (2.09 g; 9.36 mmol) was dissolved in 40 mL of anhydrous DMF under nitrogen and treated with triethylamine (2.78 mL; 20 mmol) while stirring. Ditertiarbutyl dicarbonate (3.27 g; 15 mmol) was added to the reaction mixture and stirred over night at room temperature. The solvent was removed under reduced pressure to yield a residue, which was extracted with ethyl acetate and dried with anhydrous MgSO_4 . The extraction was filtered and evaporated to give yellow oil which was purified by column chromatography on silica gel and eluted with hexane: ethyl acetate (5: 1.5 v/v). After evaporation of the solvent, yellow oil **3** was obtained. Yield: 2.00 g (6.18 mmol, 66.20%). ^1H -NMR (CDCl_3) δ = 6.97 (d, 2H, J = 8.4 Hz), 6.75 (d, 2H, J = 8.7 Hz), 4.22 (dd, 2H, J = 2.7 Hz, J = 7.2 Hz),

3.32 (dd, 2H, J = 15.0 Hz, J = 13.5), 1.55 (s, 3H), 1.48 (s, 9H), 1.32 (t, 3H, J = 18.0 Hz) ppm. ^{13}C -NMR δ = 174.16, 155.04, 154.51, 131.16, 128.50, 115.14, 77.25, 61.64, 60.54, 40.99, 28.39, 23.55, 14.77 ppm, MS: m/z = 324.36 [M] $^+$.

2.1.3. N -*t*-Butoxycarbonyl-O-[3-Hydroxypropyl]- α -Methyl Tyrosine Ethylester 4. Sodium metal (0.09 g; 14.02 mmol) was dissolved in 30 mL of anhydrous ethanol with stirring under nitrogen. Compound **3** (1.00 g; 3.09 mmol) was dissolved in 50 mL of anhydrous ethanol and treated with sodium ethoxide solution and refluxed for 2.5 h at 70°C . 3-Bromopropanol (0.56 mL; 6.18 mmol) was added and continued heating over night. The ethanol was removed under reduced pressure and replaced with 40 mL of ethyl acetate, washed with water, and dried over MgSO_4 . After removal of the solvent, it was purified by silica gel column chromatography (hexane: ethylacetate 2: 1), giving 0.83 g (2.17 mmol, 71% yield) of the product as clear yellow oil. ^1H -NMR (CDCl_3) δ = 7.01 (d, 2H, J = 6.3 Hz), 6.81 (d, 2H, J = 6.6 Hz), 4.20 (dd, 2H, J = 5.1 Hz, J = 5.1 Hz), 4.12 (t, 2H, J = 15.0 Hz), 3.86 (t, 2H, J = 10.2 Hz), 3.16 (dd, J = 13.5 Hz, J = 12.9 Hz), 2.06 (m, 2H), 1.54 (s, 3H), 1.47 (s, 9H), 1.31 (t, 3H, J = 12.3 Hz) ppm. ^{13}C -NMR δ = 174.01, 171.91, 157.73, 154.35, 131.07, 128.65, 114.14, 79.39, 65.65, 61.54, 60.40, 60.24, 40.79, 32.01, 28.39, 23.58, 14.15 ppm, MS: m/z = 381.033 [M] $^+$.

2.1.4. N -*t*-Butoxycarbonyl-O-[3-Br-Propyl]- α -Methyl Tyrosine Ethylester 5. A solution of **4** (5.44 g; 16.82 mmol) and 1,3-dibromopropane (136.74 g; 677.30 mmol) in 100 mL acetone was purged with nitrogen for 15 min. Potassium carbonate (22.62 g; 163.69 mmol) was added to the reaction mixture, the mixture was then refluxed for 12 h at 75°C . After the removal of solvents and excessive reagents under reduced pressure, the residue was dissolved in chloroform, washed with water, and dried in anhydrous magnesium sulfate. A yellow liquid was purified by silica gel flash chromatography (hexane: ethylacetate, 2: 1) to furnish compound **5** as pale yellow liquid. Yield: 4.80 g (7.52 mmol, 64.69%). ^1H -NMR (CDCl_3) δ = 7.02 (d, 2H, J = 9.00 Hz), 6.82 (d, 2H, J = 9.00 Hz), 4.23 (dd, 2H, J = 27.00), 4.09 (t, 2H, J = 12.00 Hz), 3.61 (t, 2H, J = 12.00 Hz), 3.32, 3.16 (d, 2H, J = 15.00, 12.00 Hz), 2.34 (dd, J = 24.00 Hz), 1.54 (s, 3H), 1.47 (s, 9H), 1.32 (t, 3H, J = 15.0 Hz) ppm. ^{13}C -NMR δ = 173.96, 157.63, 154.32, 131.09, 128.78, 114.18, 77.48, 65.24, 61.51, 60.35, 40.80, 30.00, 28.40, 23.60, 14.19 ppm. MS: m/z = 446.3 [M] $^+$.

2.1.5. N^1 , N^4 -Dioxylyl-1,4,8,11-Tetraazabicyclotetradecane (N^1 , N^4 -Cyclooxamide) 6. 1,4,8,11-tetraazacyclotetradecane (cyclam) (15.00 g; 74.88 mmol) was dissolved in 150 mL of anhydrous ethanol, and diethyl oxalate (10.94 g; 74.88 mmol) was added. The reaction mixture was refluxed 18 h at 75°C . The solvent was rotary evaporated, and the crude product was recrystallized in acetone: ethanol to yield white crystals of N^1 , N^4 -dioxylyl-1,4,8,11-1,5,8,12-tetraazabicyclotetradecane (N^1 , N^4 -cyclooxamide) **6**. Yield: 13.64 g (17.31 mmol, 72.00%). ^1H -NMR (CDCl_3) δ = 4.35 (m, 2H), 3.75 (m, 2H), 3.40 (m, 2H), 2.77 (m, 2H), 2.68 (m, 2H), 2.54 (m, 2H), 2.43 (m, 4H), 1.75 (m, 2H),

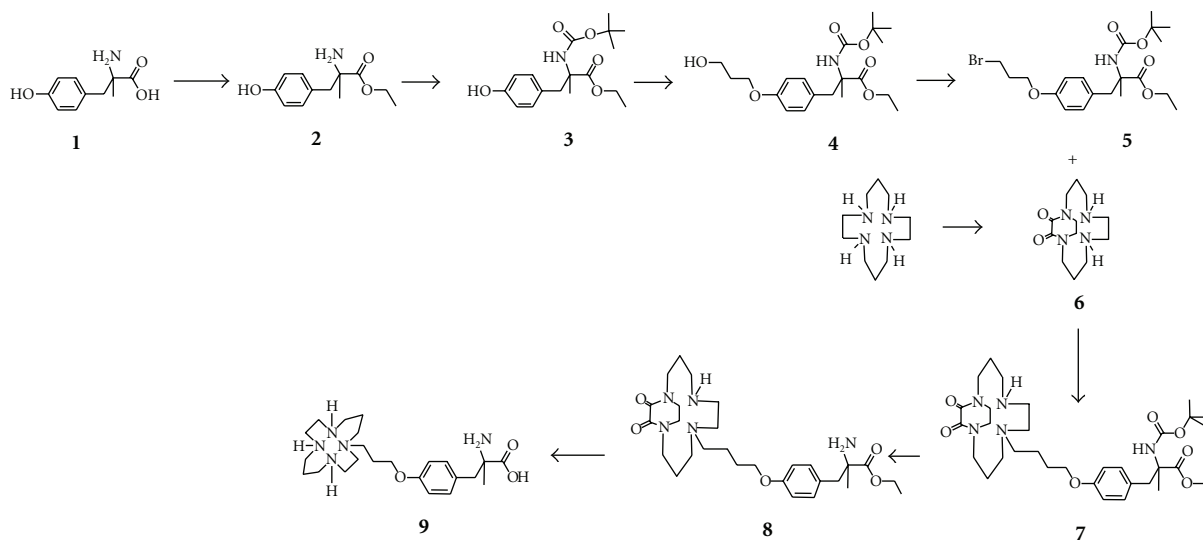


FIGURE 1: Synthetic scheme of precursor N4-AMT.

1.24 (m, 2H)) ppm. $^{13}\text{C-NMR}$ δ = 158.55, 49.92, 49.38, 47.73, 44.13, 25.42 ppm. MS: m/z = 255.33 $[\text{M}]^+$.

2.1.6. *N-t-Butoxycarbonyl-O-[3-(N^1, N^4 -Dioxylyl-1,4,8,11-Tetraazabicyclotetradecane)-Propyl]- α -Methyl Tyrosine Ethylester 7.* Compound **6** (1.00 g; 3.93 mmol) was dissolved in 20 mL of anhydrous DMF and treated with a solution of *N-t*-Butoxycarbonyl-O-[3-Br-propyl]- α -methyl tyrosine ethylester **5** (1.74 g; 3.93 mmol) in 40 mL of DMF under nitrogen atmosphere. The reaction mixture was heated to reflux for 18 h at 75°C and then allowed to cool down to room temperature. The solvent was removed *in vacuo*. The residue was dissolved in chloroform (30 mL), washed with water and 1 M Na_2CO_3 , (12 mL), and then separated for the organic layer. It was dried with anhydrous Magnesium sulfate, filtered, and evaporated. The crude compound was purified by silica gel column chromatograph (chloroform: methanol 9 : 1). Yield: 1.00 g (1.63 mmol, 42.00%). $^1\text{H-NMR}$ (CDCl_3) δ = 7.00 (d, 2H, J = 9.00 Hz), 6.79 (d, 2H, J = 9.00 Hz), 4.56 (m, 2H), 4.22 (t, 2H, J = 12.0 Hz), 3.95 (m, 2H), 3.67 (m, 2H), 3.55 (t, 2H, J = 15.0 Hz), 3.30 (m, 4H), 2.81 (m, 12H), 1.88 (m, 6H), 1.54 (s, 3H), 1.47 (s, 9H), 1.32 (t, 3H, J = 15.0 Hz) ppm. $^{13}\text{C-NMR}$ δ = 173.97, 158.65, 158.06, 157.91, 154.31, 131.01, 128.34, 114.04, 79.38, 77.27, 66.01, 61.50, 60.26, 53.76, 52.76, 49.20, 48.41, 47.54, 46.15, 45.83, 44.50, 42.60, 40.84, 28.40, 26.39, 23.57, 23.36, 23.07, 14.14 ppm. MS: m/z = 618.38 $[\text{M}]^+$.

2.1.7. *O-[3-(N^1, N^4 -Dioxylyl-1,4,8,11-Tetraazabicyclotetradecane)-Propyl]- α -Methyltyrosine Ethylester 8.* Compound **7** (0.25 g; 0.40 mmol) was dissolved in dichloromethane (10 mL), and trifluoroacetic acid (1.0 mL) was added to it. The solution was stirred over night at room temperature, and volatiles were removed *in vacuo*. The crude compound was purified by chromatography over silica gel (chloroform: methanol 9 : 1) as white solid. Yield: 0.20 g (0.39 mmol; 95.69%). $^1\text{H-NMR}$ (CD_3OD) δ = 7.14 (d, 2H, J = 9.0 Hz),

6.94 (d, 2H), 4.33 (m, 4H), 4.05 (t, 2H, J = 9.0 Hz), 3.85 (m, 2H), 3.71 (m, 2 H), 3.26 (m, 13H), 2.07 (m, 6H), 1.58 (s, 3H), 1.33 (t, 3H, J = 15.0 Hz) ppm. $^{13}\text{C-NMR}$ δ = 170.65, 161.87, 161.42, 159.70, 159.02, 158.67, 131.01, 125.14, 118.79, 114.65, 65.34, 62.47, 60.33, 56.92, 52.16, 51.26, 45.64, 45.31, 44.50, 43.20, 42.05, 24.31, 22.00, 21.39, 21.03, 16.96, 12.90 ppm, MS: m/z = 517.63 $[\text{M}]^+$.

2.1.8. *O-[3-(1,4,8,11-Tetraazabicyclohexadecane)-Propyl]- α -Methyl Tyrosine (N_4 -AMT) 9.* To a solution of compound **8** (0.20 g; 0.39 mmol) in a 5 mL of water, 10 N NaOH (2 mL) was added, stirred, and refluxed over night at 90°C. The solvent was evaporated under vacuum, giving white solid, which was dissolved in 5 mL of water and neutralized with 5 N HCl solution to pH = 7. It was lyophilized and obtained as white solid. The solid was stirred in 25 mL anhydrous methanol, filtered, and evaporated to afford an off white solid. Yield: 0.20 g (0.46 mmol: 99.0%). $^1\text{H-NMR}$ (D_2O) δ = 7.21 (d, 2H, J = 9.00 Hz), 7.00 (d, 2H, J = 9.00 Hz), 4.14 (t, 2H, J = 12.0 Hz), 3.10 (m, 5H), 2.94 (m, 2H), 2.84 (m, 13H), 1.95 (m, 6H), 1.33 (s, 3H) ppm. $^{13}\text{C-NMR}$ δ = 180.69, 163.42, 163.16, 162.88, 162.60, 157.06, 131.40, 129.19, 117.57, 115.26, 115.10, 112.93, 66.25, 60.73, 53.69, 51.46, 49.88, 49.26, 48.04, 47.84, 46.60, 45.42, 45.07, 43.94, 24.71, 24.32, 23.62, 22.55 ppm. MS: m/z = 436.327 $[\text{M}]^+$.

2.2. Radiosynthesis of $^{99\text{m}}\text{Tc-N}_4\text{-AMT}$. Radiolabeling of $N_4\text{-AMT}$ with $^{99\text{m}}\text{Tc}$ was performed in a standard manner [14]. Briefly, radiosynthesis of $^{99\text{m}}\text{Tc-N}_4\text{-AMT}$ was achieved by adding a required amount of sodium pertechnetate into a vial containing precursor $N_4\text{-AMT}$ and SnCl_2 (100 μg). Radiochemical purity was assessed by high-performance liquid chromatography (HPLC), equipped with NaI and UV detector (274 nm), and was performed using a C-18 reverse column with a mobile phase of acetonitrile : water (7 : 3) at a flow rate of 0.5 mL/min.

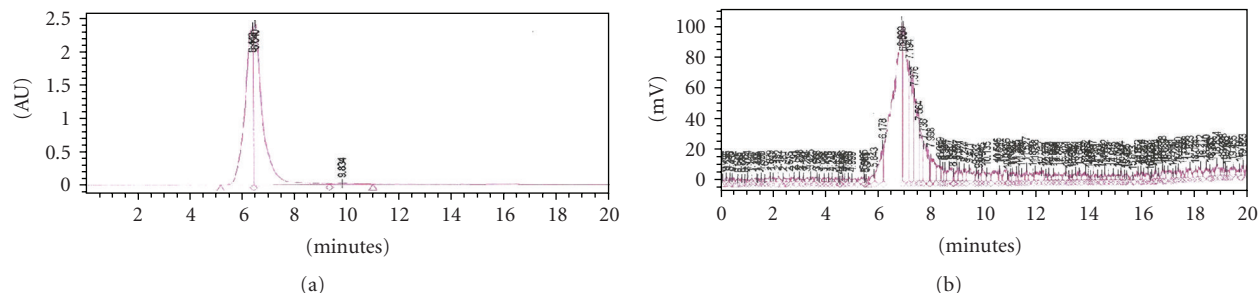


FIGURE 2: HPLC analysis of ^{99m}Tc -N4-AMT at a flow rate of 0.5 mL/min using a C-18 reverse column under UV absorbance of 274 nm.

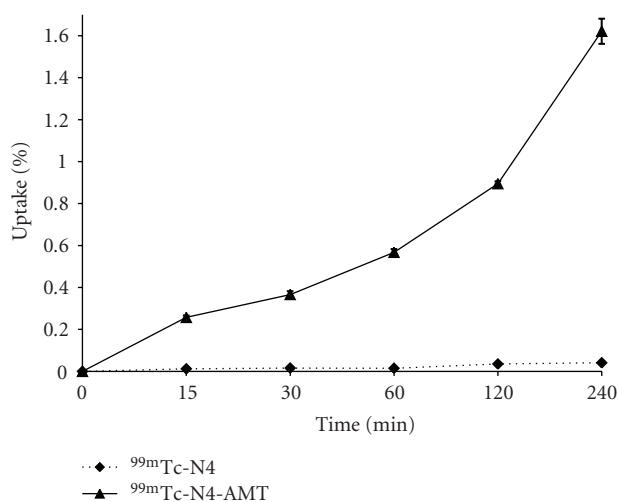


FIGURE 3: *In vitro* cellular uptake of ^{99m}Tc -N4-AMT. The cellular uptake kinetics of ^{99m}Tc -N4-AMT and ^{99m}Tc -N4 was conducted in the rat breast tumor cell line 13762. Data were expressed in mean \pm S.D. percent of cellular uptake (%Uptake).

2.3. *In Vitro* Cellular Uptake of ^{99m}Tc -N4-AMT. Rat mammary tumor cell line 13762 was obtained from American Type Culture Collection (Rockville, MD). The same cell line was used to create the animal model for *in vivo* evaluation. Cells were maintained at 37°C in a humidified atmosphere containing 5% CO₂ in Dulbecco's modified Eagle's medium and nutrient mixture F-12 Ham (DMEM/F12; GIBCO, Grand Island, NY). Cells were plated to 6-well tissue culture plates (2×10^5 cells/well) for two days before the study, and incubated with ^{99m}Tc -N4-AMT (0.05 mg/well, 8 μCi /well) or ^{99m}Tc -N4 chelator itself (0.025 mg/well, 8 μCi /well) for 15 min–4 h. After incubation, cells were washed with ice-cold PBS twice and detached by adding 0.5 mL of trypsin. Cells were then collected and the radioactivity was measured with gamma counter (Cobra Quantum; Packard, MN). Data was expressed in mean \pm S.D. percent of cellular uptake.

2.4. *In Vivo* Tissue Distribution Studies. All animal work was carried out in the Small Animal Imaging Facility (SAIF) at University of Texas MD Anderson Cancer Center under the protocol approved by Institutional Animal Care and Use

Committee (IACUC). Tissue distribution studies of ^{99m}Tc -N4-AMT (study I, $n = 9$) or ^{99m}Tc -N4 (study II, $n = 9$) were conducted by using normal female Fischer 344 rats (150 ± 25 g, $n = 18$) (Harlan Sprague-Dawley, Indianapolis, IN). For each radiotracer, nine rats were divided into three groups for three time intervals (0.5, 2, 4 h). The injection activity was $25 \pm 0.5 \mu\text{Ci}$ /rat intravenously. At each time interval, the rats were sacrificed, and the selected tissues were excised, weighed, and measured for radioactivity by gamma counter. Data from each sample were represented as the percentage of the injected dose per gram of tissue wet weight (%ID/g). Counts from a diluted sample of the original injection were used as the reference.

2.5. Planar Scintigraphic Imaging Studies of ^{99m}Tc -N4-AMT. Female Fischer 344 rats were inoculated subcutaneously with 0.1 mL of 13762 rat mammary tumor cell suspension (10^5 cells/rat) into the right posterior legs using 22-gauge needles. Imaging studies were performed 14 to 17 days after inoculation when tumors reached approximately 1 cm in diameter. The anesthetized rats were injected intravenously with ^{99m}Tc -N4-AMT (0.3 mg/rat, 300 μCi /rat; $n = 3$) or with ^{99m}Tc -N4 (0.15 mg/rat, 300 μCi /rat; $n = 3$), respectively. Planar scintigraphic images were obtained using M-CAM (Siemens Medical Solutions, Hoffman Estates, IL) equipped with a Low-Energy High-Resolution collimator at 30–120 min. The field of view was 53.3 cm \times 38.7 cm. The intrinsic spatial resolution was 3.2 mm and the pixel size was from 19.18 mm (32×32 , zoom = 1) to 0.187 mm (1024×1024 , zoom = 3.2). Computer outlined regions of interest (ROI) (counts per pixel) of tumors, and normal muscle tissues at symmetric sites were used to calculate tumor-to-muscle (T/M) ratios.

3. Results and Discussion

3.1. Chemistry. N4-AMT was synthesized via an eight-step procedure (Figure 1). Commercially available α -methyl tyrosine 1 was converted into corresponding acid chloride, then to ethyl ester by reacting with thionyl chloride in ethanol. The amine in α -methyl tyrosine ethyl ester 2 was protected as its Boc-derivative N-t-butoxycarbonyl- α -methyl tyrosine ethylester 3 with triethylamine and di-*t*-butyldicarbonate in DMF. The chain at the –OH group was extended when compound

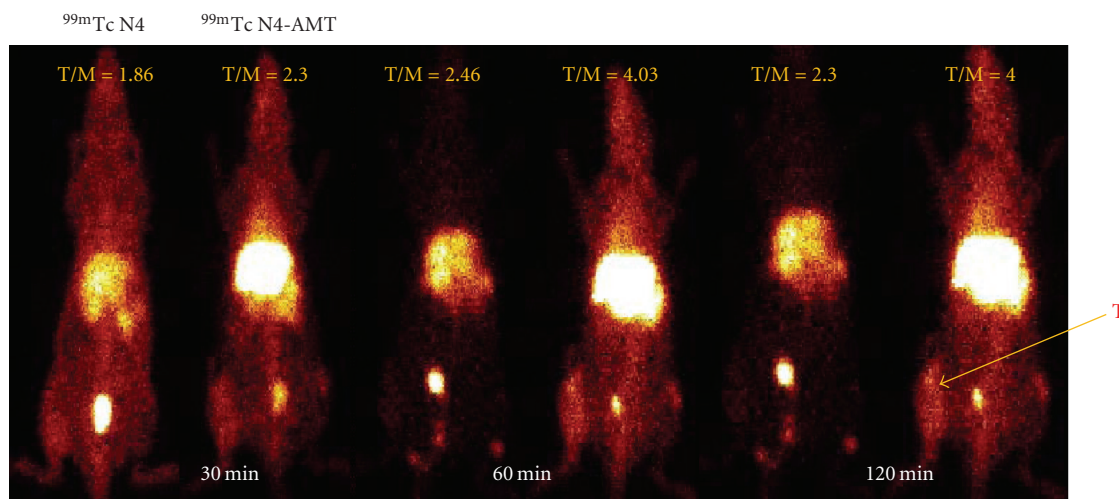


FIGURE 4: Planar scintigraphic imaging studies of $^{99m}\text{Tc-N}_4\text{-AMT}$. Scintigraphic images of Fisher 344 tumor bearing rats were acquired, and computer outlined regions of interest (counts per pixel) in the tumors (T) and the symmetrical muscle tissues (M) were used to determine T/M count density ratios.

3 was treated with 1, 3-dibromopropane and obtained as N-t-butoxycarbonyl-O-[3-bromopropyl]- α -methyl tyrosine ethylester 4. Acylation of 1,4,8,11-tetraazacyclo-tetradecane (cyclam) with diethyloxalate led to N^1, N^4 -dioxalyl 1,4,8,11-tetraazacyclotetradecane (N^1, N^4 -cyclamoxamide) 5. Under SN^2 condition 4 and 5 were efficiently converted to alkylated compound N-t-butoxycarbonyl-O-[3-(N^1, N^4 -dioxalyl-1,4,8,11-tetraazacyclotetradecane)-propyl]- α -methyl tyrosine ethylester 6. Exposure of 6 to trifluoroacetic acid in CH_2Cl_2 caused qualitative de-t-butoxycarboxylation to yield O-[3-(N^1, N^4 -dioxalyl 1,4,8,11-tetraazacyclotetradecane)-propyl]- α -methyl tyrosine ethylester 7. 10 N NaOH in water at 75°C promoted the hydrolysis of ester to acid and a simultaneous deoalation of 7 to yield the final compound O-[3-(1,4,8,11-tetraazacyclotetradecan)-propyl]- α -methyl tyrosine ($\text{N}_4\text{-AMT}$) 8. The total synthesis yield was 14%, which can be adapted to industrial manufacturing. The structure and purity of the compounds at each step were validated by ^1H - and ^{13}C -NMR, mass spectra, and HPLC.

3.2. Radiosynthesis. As shown in Figure 2, precursor $\text{N}_4\text{-AMT}$ could be labeled with ^{99m}Tc successfully in a high radiochemical purity (>96%). The retention time of $^{99m}\text{Tc-N}_4\text{-AMT}$ was 6.899 min. Given that $^{99m}\text{Tc-N}_4\text{-AMT}$ is a kit-product and labeled without any further purification, the radiochemical yield was assumed to be identical to its radiochemical purity. In this study, we labeled amino acid α -methyltyrosine AMT with ^{99m}Tc using cyclam N_4 as the chelator because of its stable chelating ability and fast renal clearance. ^{99m}Tc was selected as the radionuclide due to its favorable physical characteristics, suitable half-life, and cost-effectiveness.

3.3. In Vitro Cellular Uptake of $^{99m}\text{Tc-N}_4\text{-AMT}$. The cellular uptake kinetics of $^{99m}\text{Tc-N}_4\text{-AMT}$ and $^{99m}\text{Tc-N}_4$ in rat breast tumor cell line 13762 is shown in Figure 3. There

was a drastically increased uptake for $^{99m}\text{Tc-N}_4\text{-AMT}$ in the tumor cells at 15–240 min, but not for $^{99m}\text{Tc-N}_4$ chelator. These findings suggest that by adding the amino acid AMT, $^{99m}\text{Tc-N}_4\text{-AMT}$ can enter and accumulate into tumor cells effectively and rapidly. To further investigate the transport mechanisms of $^{99m}\text{Tc-N}_4\text{-AMT}$, the competitive inhibition study using various types of transporter inhibitors will be conducted in the future.

3.4. In Vivo Evaluation of $^{99m}\text{Tc-N}_4\text{-AMT}$. The result of the *in vivo* biodistribution studies in the normal Fischer rats at 0.5, 2, and 4 hours after intravenous administration of $^{99m}\text{Tc-N}_4\text{-AMT}$ is shown in Table 1. Planar scintigraphic images of $^{99m}\text{Tc-N}_4\text{-AMT}$ and $^{99m}\text{Tc-N}_4$ at 30, 60, and 120 min in breast tumor-bearing rats are shown in Figure 4. T/M ratios of $^{99m}\text{Tc-N}_4\text{-AMT}$ were 2.3–4.0, whereas those of $^{99m}\text{Tc-N}_4$ were 1.9–2.5, respectively. Tumors could be clearly visualized by $^{99m}\text{Tc-N}_4\text{-AMT}$, but not by $^{99m}\text{Tc-N}_4$. In addition, the rat kidneys showed intense activity of $^{99m}\text{Tc-N}_4\text{-AMT}$ in the planar images, which was consistent with the results from the *in vivo* biodistribution studies in the normal rats. This may be due to the nature of AMT, an inhibitor of tyrosine hydroxylase that cannot be excreted from kidneys and hence crystallized in the proximal tubules because of its poor solubility at the hydrogen ion concentrations of body fluids (pH 5–8) [15]. In the future, *in vivo* uptake blocking study using the unlabeled AMT will be performed to ascertain whether accumulation of $^{99m}\text{Tc-N}_4\text{-AMT}$ in the kidney is attributed to AMT module.

4. Conclusion

In conclusion, efficient synthesis of $\text{N}_4\text{-AMT}$ was achieved. *In vitro* cellular uptake and *in vivo* imaging findings collectively suggest that $^{99m}\text{Tc-N}_4\text{-AMT}$ is a potential radiotracer for breast cancer imaging. In compliance with the chelating

TABLE 1: Biodistribution of ^{99m}Tc -N4-AMT in Normal Fischer 344 Rats.

	30 MIN	120 MIN	240 MIN
blood	0.74 ± 0.024	0.28 ± 0.010	0.18 ± 0.008
heart	0.18 ± 0.013	0.08 ± 0.006	0.05 ± 0.003
lung	0.44 ± 0.029	0.22 ± 0.004	0.13 ± 0.008
thyroid	0.57 ± 0.040	0.31 ± 0.015	0.24 ± 0.012
pancreas	0.18 ± 0.006	0.09 ± 0.005	0.06 ± 0.002
liver	1.40 ± 0.077	0.83 ± 0.045	0.60 ± 0.023
spleen	0.24 ± 0.004	0.19 ± 0.002	0.18 ± 0.011
kidney	5.77 ± 0.355	5.32 ± 0.180	4.74 ± 0.332
stomach	0.50 ± 0.029	0.42 ± 0.031	0.43 ± 0.026
intestine	0.33 ± 0.019	0.18 ± 0.010	0.13 ± 0.006
uterus	0.34 ± 0.014	0.14 ± 0.023	0.08 ± 0.004
muscle	0.09 ± 0.007	0.03 ± 0.002	0.02 ± 0.001
bone & joint	0.27 ± 0.061	0.11 ± 0.006	0.06 ± 0.003
brain	0.03 ± 0.005	0.01 ± 0.001	0.01 ± 0.000

Each value is the percentage of injected dose per gram weight ($n = 3$)/time interval. Each datum represents the mean of three measurements with standard deviation.

capability of N4, N4-AMT could be labeled with positron emitting radionuclides such as Gallium-68 or with short-ranged beta emitters for internal radiotherapeutic purposes hereafter.

Authors' Contribution

Fan-Lin Kong and Mohammad S. Ali contributed equally to this work.

Acknowledgments

The research was funded by Cell>Point company (Inglewood, CO) under MDA SRA LS2005-00012803PL. The NMR, mass spectrometry, and animal research are supported by M. D. Anderson Cancer Center (CORE) Grant NIH CA-16672.

References

- [1] A. Buerkle and W. A. Weber, "Imaging of tumor glucose utilization with positron emission tomography," *Cancer and Metastasis Reviews*, vol. 27, no. 4, pp. 545–554, 2008.
- [2] G. Yamaura, T. Yoshioka, H. Fukuda et al., "O-[18F]fluoromethyl-L-tyrosine is a potential tracer for monitoring tumour response to chemotherapy using PET: an initial comparative in vivo study with deoxyglucose and thymidine," *European Journal of Nuclear Medicine and Molecular Imaging*, vol. 33, no. 10, pp. 1134–1139, 2006.
- [3] E. M. del Amo, A. Urtti, and M. Yliperttula, "Pharmacokinetic role of L-type amino acid transporters LAT1 and LAT2," *European Journal of Pharmaceutical Sciences*, vol. 35, no. 3, pp. 161–174, 2008.
- [4] H. Yagita, T. Masuko, and Y. Hashimoto, "Inhibition of tumor cell growth in vitro by murine monoclonal antibodies that recognize a proliferation-associated cell surface antigen system in rats and humans," *Cancer Research*, vol. 46, no. 3, pp. 1478–1484, 1986.
- [5] T. Sakata, G. Ferdous, T. Tsuruta et al., "L-type amino-acid transporter 1 as a novel biomarker for high-grade malignancy in prostate cancer," *Pathology International*, vol. 59, no. 1, pp. 7–18, 2009.
- [6] G. Mariani, L. Bruselli, and A. Duatti, "Is PET always an advantage versus planar and SPECT imaging?" *European Journal of Nuclear Medicine and Molecular Imaging*, vol. 35, no. 8, pp. 1560–1565, 2008.
- [7] N. R. Schechter, D. J. Yang, A. Azhdarinia, and M. Chanda, "Technologies for translational imaging using generators in oncology," *Recent Patents on Anti-Cancer Drug Discovery*, vol. 2, no. 3, pp. 251–258, 2007.
- [8] S. Liu, "The role of coordination chemistry in the development of target-specific radiopharmaceuticals," *Chemical Society Reviews*, vol. 33, no. 7, pp. 445–461, 2004.
- [9] S. Liu, "Bifunctional coupling agents for radiolabeling of biomolecules and target-specific delivery of metallic radionuclides," *Advanced Drug Delivery Reviews*, vol. 60, no. 12, pp. 1347–1370, 2008.
- [10] K. Ohtsuki, K. Akashi, Y. Aoka et al., "Technetium-99m HYNIC-annexin V: a potential radiopharmaceutical for the in-vivo detection of apoptosis," *European Journal of Nuclear Medicine*, vol. 26, no. 10, pp. 1251–1258, 1999.
- [11] C. G. Van Nerom, G. M. Bormans, M. J. De Roo, and A. M. Verbruggen, "First experience in healthy volunteers with technetium-99m L,L-ethylenedicycysteine, a new renal imaging agent," *European Journal of Nuclear Medicine*, vol. 20, no. 9, pp. 738–746, 1993.
- [12] C. H. Kao, S. P. ChangLai, P. U. Chieng, and T. C. Yen, "Technetium-99m methoxyisobutylisonitrile chest imaging of small cell lung carcinoma: relation to patient prognosis and chemotherapy response—a preliminary report," *Cancer*, vol. 83, no. 1, pp. 64–68, 1998.
- [13] H. C. Wu, C. H. Chang, M. M. Lai, C. C. Lin, C. C. Lee, and A. Kao, "Using Tc-99m DMSA renal cortex scan to detect renal damage in women with type 2 diabetes," *Journal of Diabetes and Its Complications*, vol. 17, no. 5, pp. 297–300, 2003.
- [14] A. Barth, A. R. Haldemann, J. C. Reubi et al., "Noninvasive differentiation of meningiomas from other brain tumours using combined Indium-octreotide/technetium-DTPA brain

scintigraphy," *Acta Neurochirurgica*, vol. 138, no. 10, pp. 1179–1185, 1996.

- [15] K. E. Moore, P. F. Wright, and J. K. Bert, "Toxicologic studies with alpha-methyltyrosine, an inhibitor of tyrosine hydroxylase," *Journal of Pharmacology and Experimental Therapeutics*, vol. 155, no. 3, pp. 506–515, 1967.